

Fig. 2 UV melting curves of tandem duplexes. Solid and broken curves show the meltings of $\text{CyD-ODN}_1/\text{target27}/\text{Fc-ODN}_1$ and $\text{CyD-ODN}_1/\text{target27}/\text{ODN20}$, respectively. Melting experiments were carried out in 10 mM phosphate buffer solution (pH 7.0) containing 500 mM KCl. The concentrations of the ODN components were all 1.0 μM . The solutions were heated at a rate of 0.5 $^\circ\text{C min}^{-1}$. Inset shows the fitting of the melting at lower temperature to the theoretical curve. Closed and open circles are the experimental data for each tandem duplex. Red curves are the optimized theoretical curves.

attributed to those of 7-mer and 20-mer ODNs, respectively.^{11a} Fig. 2 shows the melting curves of the tandem duplexes $\text{CyD-ODN}_1/\text{target27}/\text{Fc-ODN}_1$ and $\text{CyD-ODN}_1/\text{target27}/\text{ODN20}$. The T_{max} of CyD-ODN_1 dissociation from $\text{CyD-ODN}_1/\text{target27}/\text{Fc-ODN}_1$ was higher than that for $\text{CyD-ODN}_1/\text{target27}/\text{ODN20}$. The difference in the T_{max} values was almost 20 $^\circ\text{C}$. This could be attributed to the stabilization effect of the interaction between βCyD and Fc on the tandem duplex. The lower temperature regions of both melting curves were fitted with the theoretical equation (Fig. 2, inset).^{3a,12} The thermodynamic parameters obtained and the T_{max} values of all the tandem duplexes are summarized in Table 1. The difference in ΔG_{298}° for CyD-ODN_1 binding with $\text{target27}/\text{Fc-ODN}_1$ and with $\text{target27}/\text{ODN20}$ ($\Delta\Delta G^\circ$) was ca. 3.2 kcal mol $^{-1}$. This is a reasonable value as the free energy comes from the formation of a $\beta\text{CyD-Fc}$ inclusion complex.^{7,13} This corresponds to an enhancement by ca. 260 times of the binding constant at 25 $^\circ\text{C}$. This means that the βCyD tethered to the ODN end accommodates the Fc tethered to the neighboring end of another ODN on the target DNA to form a tight inclusion complex without significant strain in the structure.

The electrochemical properties of Fc-ODN_1 were investigated by cyclic voltammetry using a dual microelectrode. Fig. 3(a) shows the cyclic voltammograms of Fc-ODN_1 in several states. The current based on the ferrocene/ferrocenium

Table 1 Melting temperatures^a and thermodynamic parameters^b of duplex formation

Tandem duplex with target27	$T_{\text{max}}/^\circ\text{C}$		$\Delta G_{298}^\circ/\text{kcal mol}^{-1}$	$K_{298}/\text{mol L}^{-1}$
	Lower	Higher		
$\text{CyD-ODN}_1/\text{Fc-ODN}_1$	37.4	73.5	-10.6	6.52×10^7
$\text{ODN7}/\text{Fc-ODN}_1$	19.7	73.4		
$\text{CyD-ODN}_1/\text{ODN20}$	18.7	73.9	-7.36	2.50×10^5
$\text{ODN7}/\text{ODN20}$	24.1	73.5		

^a The temperatures of biphasic UV inflections. Higher and lower temperatures of two maxima of 1st derivative curves are shown as $T_{\text{max},s}$.^b ΔH° and ΔS° for duplex formation of CyD-ODN_1 with half duplexes are shown in ESI†. ΔG° and K were calculated from them at 298 K.

redox couple (Fc/Fc^+) was significantly suppressed only for the ternary tandem duplex $\text{CyD-ODN}_1/\text{target27}/\text{Fc-ODN}_1$. As we expected, the electrochemical activity of Fc in the DNA conjugate seems to be significantly quenched by shielding with βCyD on the DNA scaffold. βCyD as an intervening aliphatic insulator would prevent the Fc from reaching the electrode directly and would suppress the rate of electron transfer. The difficulty in accessing the counter anion experienced by ferrocenium tightly surrounded by βCyD might be another cause of the current suppression. Recently, several electrochemical methods for DNA analysis have been proposed based on $\beta\text{CyD-Fc}$ interactions.¹⁴ The contrasts in the magnitude of the electric currents obtained in the present study are much higher than those previously reported. This might be the result of differences in the linker chains such as the length, structure, and tethering point on βCyD , which would significantly affect the structure and stability of the inclusion complexes (ESI†).

The effects of the sequence of the target DNAs on the current based on Fc/Fc^+ were examined using the system of tandem duplex 2 with the four targets, i.e., **target22N** carrying one base displacement. Square-wave voltammograms measured at 40 $^\circ\text{C}$ are shown in Fig. 3(b). UV melting experiments for these four tandem duplexes, $\text{CyD-ODN}_2/\text{target22N}/\text{Fc-ODN}_2$, showed that only **target22C** can form a stable tandem duplex at this temperature (ESI†). As we expected, only the signal from the duplex $\text{CyD-ODN}_2/\text{target22C}/\text{Fc-ODN}_2$ almost vanished. The current signal increased with increasing temperature. Then, finally, it gave almost the same magnitude as those of the other three duplexes at 55 $^\circ\text{C}$ (ESI†). This result clearly shows that the $\beta\text{CyD-Fc}$ inclusion complex formation is controlled by sequence-specific hybridization of ODNs. Control of the interaction is not difficult by taking advantage of the programmability and the predictable thermal stability of DNA structures.¹⁵

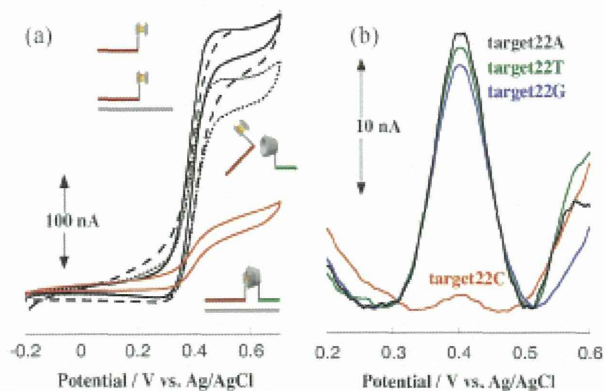


Fig. 3 Electrochemical responses of Fc-ODN in several states. (a) Cyclic voltammograms performed with dual-mode techniques using a pair of comb-shaped working electrodes (collector and generator) at 5 $^\circ\text{C}$. A 15 μL solution containing the DNA components (100 μM), 10 mM phosphate buffer (pH 7.0), and 500 mM KCl was dropped on the electrodes. Scan rate of generator: 10 mV s^{-1} ; collector potential: -0.2 V (vs. Ag/AgCl). Solid curve in black: Fc-ODN_1 ; broken curve: $\text{target27}/\text{Fc-ODN}_1$; dotted curve: $\text{CyD-ODN}_1/\text{Fc-ODN}_1$; red curve: $\text{CyD-ODN}_1/\text{target27}/\text{Fc-ODN}_1$. (b) Square-wave voltammograms of $\text{CyD-ODN}_2/\text{target22N}/\text{Fc-ODN}_2$. A 50 μL solution containing the DNA components (20 μM), 10 mM phosphate buffer (pH 7.0), and 500 mM KCl was subjected to measurements at 40 $^\circ\text{C}$. Amplitude: 25 mV; potential increment: 4 mV; frequency: 15 Hz. Red: **target22C**; blue: **target22G**; green: **target22T**; black: **target22A**.

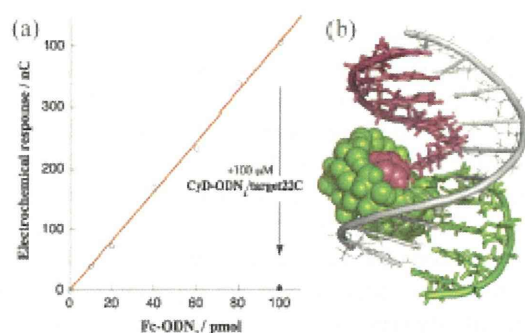


Fig. 4 Switching the electrochemical signal of Fe-ODN by specific interaction with CyD-ODN. (a) Linear calibration of the electrochemical response of Fe-ODN₂ (open circle) and its quenched signal (closed circle) obtained by a flow system at 25 °C. Twenty μL of standard solutions containing various amounts of Fe-ODN₂, 10 mM phosphate buffer (pH 7.0), and 500 mM KCl were injected into the HPLC-ECD. To the solution containing 100 pmol Fe-ODN₂, an equimolar amount of CyD-ODN₂/target22C was added and its signal was measured as that of the quenched state. Eluent: 100 mM phosphate buffer (pH 7.0), 750 mM NaCl, 5 mg mL⁻¹ EDTA; potential: 500 mV (vs. Ag/AgCl); § flow rate: 1.0 mL min⁻¹; column: Inertsil AX (4.6 φ × 100 mm). (b) One of the possible structures of the ternary tandem duplex (only the central part of duplex 2). Red: Fe-ODN₂, green: CyD-ODN₂, gray: target22C. The model was geometry-optimized by AMBER* force field with the GB/SA (generalized Born/surface area) solvent model using MacroModel version 9.1.

The sensitivity of SWV was not sufficient. Therefore, system 2 was subjected to flow analysis to check the applicability of the system for practical use. HPLC equipped with an electrochemical detector (ECD) was used. Fig. 4(a) shows the calibration profile of the electrochemical response of Fe-ODN₂ and its complex form. Without taking any special care, 10 pmol per 20 μL of Fe-ODN₂ were detected with fair reproducibility by amperometry using ordinary ECD. It would not be difficult to improve the sensitivity by reviewing some of the parameters of the flow system such as type of column, flow rate, and eluent. The performance we achieved was reasonable for this concise procedure, in which all we did was mix and inject the components. As observed in the voltammograms of static solutions shown in Fig. 3 and 4, the current signal was almost perfectly suppressed by stoichiometric complexation with CyD-ODN₂ in the flow system. This shows that the tandem duplex is stable, and Fc would be steadily buried in βCyD and shielded from the bulk solution (Fig. 4(b)), even under the conditions of HPLC-ECD. Thus, the present system could be applied to flow analysis without any modification of the system architecture. Good compatibility with flow analyses is one of the advantages of systems that work in homogeneous solutions⁹ because, generally, flow analyses enable quick and reproducible measurements to be made, and lead directly to applications in the micro total analyses such as μTAS or lab-on-a-chip.¹⁶

In conclusion, we have shown that the electrochemical activity of Fc is controlled reversibly by a designed interaction with βCyD on a DNA scaffold. βCyD could be regarded as an effective quencher for Fc. This would free the design of the molecular sensor from the need for electrode modification of

one of the counterparts of the specific interactions of interest. The system configuration is general and could be extended as a common design strategy for electrochemical molecular sensing, that is, the targets are not limited to tandem duplexes or even DNA-based molecular systems.

This work was partially supported by a Grant-in-Aid for Scientific Research on Innovative Areas ("Coordinating Programming" Area 2107, No. 22108529) from MEXT (T.I.), Scientific Research (B) (20350038) from JSPS (T.I.).

Notes and references

‡ Melting temperature, T_m , is usually defined as the temperature at which half of the ODN exists in the duplex state and the other half in the single-stranded state.¹² For the sake of convenience, here the temperatures that give maximum of 1st derivative curves were used as the measure for thermal stability of the duplexes.

§ To determine the applied potential, hydrodynamic voltammeteries were carried out prior to conducting calibration using the same HPLC-ECD system (ESI†).^{3b}

- For example, *Electrochemistry of Functional Supramolecular Systems*, ed. P. Ceroni, A. Credi and M. Venturi, Wiley, Hoboken, 2010.
- (a) E. M. Boon, J. E. Salas and J. K. Barton, *Nat. Biotechnol.*, 2002, **20**, 282; (b) E. Farjami, L. Clima, K. Gothelf and E. E. Ferapontova, *Anal. Chem.*, 2011, **83**, 1594; (c) Y. Xiao, X. Qu, K. W. Plaxco and A. J. Heeger, *J. Am. Chem. Soc.*, 2007, **129**, 11896; (d) Y. Xiang, X. Qian, B. Jiang, Y. Chai and R. Yuan, *Chem. Commun.*, 2011, **47**, 4733.
- (a) T. Ihara, Y. Maruo, S. Takenaka and M. Takagi, *Nucleic Acids Res.*, 1996, **24**, 4273; (b) S. Takenaka, Y. Uto, H. Kondo, T. Ihara and M. Takagi, *Anal. Biochem.*, 1994, **218**, 436; (c) S. Takenaka, T. Ihara and M. Takagi, *J. Chem. Soc., Chem. Commun.*, 1990, 1485; (d) T. Ihara, D. Sasahara, M. Shimizu and A. Jyo, *Supramol. Chem.*, 2009, **21**, 207.
- (a) T. Ihara, M. Nakayama, M. Murata, K. Nakano and M. Maeda, *Chem. Commun.*, 1997, 1609; (b) M. Nakayama, T. Ihara, K. Nakano and M. Maeda, *Talanta*, 2002, **56**, 857.
- (a) T. Ihara, A. Uemura, A. Futamura, M. Shimizu, N. Baba, S. Nishizawa, N. Teramae and A. Jyo, *J. Am. Chem. Soc.*, 2009, **131**, 1386; (b) D. B. Harris, B. R. Saks and J. Jayawickramarajah, *J. Am. Chem. Soc.*, 2011, **133**, 7676.
- A. Kuzuya, T. Ohnishi, T. Wasano, S. Nagaoka, J. Sumaoka, T. Ihara, A. Jyo and M. Komiyama, *Bioconjugate Chem.*, 2009, **20**, 1643.
- (a) D. R. van Staveren and N. Metzler-Nolte, *Chem. Rev.*, 2004, **104**, 5931; (b) T. Matsue, D. H. Evans, T. Osa and N. Kobayashi, *J. Am. Chem. Soc.*, 1985, **107**, 3411.
- For example, R. T. Ranasinghe and T. Brown, *Chem. Commun.*, 2005, 5487.
- T. Ihara and M. Mukae, *Anal. Sci.*, 2007, **23**, 625.
- E. Y. Krynetski, J. D. Schuetz, A. J. Galpin, C.-H. Pui, M. V. Relling and W. E. Evans, *Proc. Natl. Acad. Sci. U. S. A.*, 1995, **92**, 949.
- (a) D. M. Kolpashchikov, *Chem. Rev.*, 2010, **110**, 4709; (b) Y. Kitamura, T. Ihara, Y. Tsujimura, Y. Osawa, D. Sasahara, M. Yamamoto, K. Okada, M. Tazaki and A. Jyo, *J. Inorg. Biochem.*, 2008, **102**, 1921.
- (a) L. A. Marky and K. J. Breslauer, *Biopolymers*, 1987, **26**, 1601; (b) M. Petersheim and D. H. Turner, *Biochemistry*, 1983, **22**, 256.
- (a) F. Hapiot, S. Tilloy and E. Monflier, *Chem. Rev.*, 2005, **106**, 767; (b) L. J. Prins and P. Scimin, *Angew. Chem., Int. Ed.*, 2009, **48**, 2288.
- (a) H. Aoki, A. Kitajima and H. Tao, *Supramol. Chem.*, 2010, **22**, 455; (b) S. Sato, T. Nojima and S. Takenaka, *Organomet. Chem.*, 2004, **689**, 4722.
- For example, M. Zuker, *Nucleic Acids Res.*, 2003, **31**, 3406.
- For example, *Nanobiotechnology, Concepts, Applications and Perspectives*, ed. C. M. Niemeyer and C. Mirkin, Wiley-VCH, Weinheim, 2004.

